
Glycobiology and Extracellular Matrices:

# N-glycan Remodeling on Glucagon Receptor is an Effector of Nutrient-sensing by the Hexosamine Biosynthesis Pathway

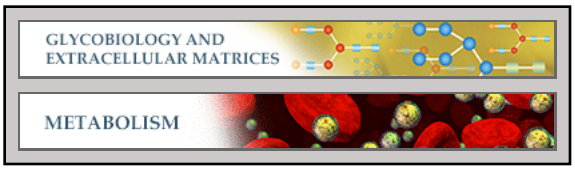


Anita Johswich, Christine Longuet, Judy Pawling, Anas Abdel Rahman, Michael Ryczko, Daniel J. Drucker and James W. Dennis

*J. Biol. Chem.* *published online April 17, 2014*

---

Access the most updated version of this article at doi: 10.1074/jbc.M114.563734

JBC Papers in Press. Published on April 17, 2014 as Manuscript M114.563734
The latest version is at http://www.jbc.org/cgi/doi/10.1074/jbc.M114.563734


# N-glycan remodeling on glucagon receptor is an effector of nutrient-sensing by the hexosamine biosynthesis pathway*

**Anita Johswich[1], Christine Longuet[1], Judy Pawling[1], Anas Abdel Rahman[1], Michael Ryczko[1,2], Daniel J. Drucker[1,3] and James W. Dennis[1,2,3]**

1. Lunenfeld-Tanenbaum Research Institute, Mount Sinai Hospital, 600 University Avenue R988, Toronto, Ontario, Canada M5G 1X5
2. Department of Molecular Genetics, & Department of Laboratory Medicine and Pathology,
3. Department of Medicine, University of Toronto

***Running title:** *N-glycan remodeling on glucagon receptor*

To whom correspondence should be addressed: James W. Dennis, Lunenfeld Tanenbaum Research Institute, Mount Sinai Hospital, 600 University Avenue, R988, Toronto, Ontario, Canada, M5G1X5 Tel: 416-586-8233; FAX: 416-586-8587. Email: dennis@lunenfeld.ca

**Keywords:** Metabolism, glucagon receptor, Golgi N-acetylglucosaminyltransferases, Mgat5

---

**Background**: The hexosamine biosynthesis pathway to UDP-GlcNAc has been implicated in glucose homeostasis.
**Results:** UDP-GlcNAc and Golgi N-acetylglucosaminyltransferases modify the N-glycans on glucagon receptor, which increases sensitivity to glucagon *in vivo*.
**Conclusion**: The hexosamine biosynthesis pathway contributes to glucose homeostasis, in part, through N-glycan branching on glucagon receptor.
**Significance**: Hepatic Mgat5 and the N-glycan branching pathway may be a therapeutic target for control of glycemia.

---

## ABSTRACT

Glucose homeostasis in mammals is dependent on the opposing actions of insulin and glucagon. The Golgi N-acetylglucosaminyltransferases encoded by Mgat1, Mgat2, Mgat4a/b/c and Mgat5 modify the N-glycans on receptors and solute transporter, possibly adapting activities in response to the metabolic environment. Herein we report that Mgat5$^{-/-}$ mice display diminished glycemic response to exogenous glucagon, together with increased insulin sensitivity. Glucagon receptor signaling and gluconeogenesis in *Mgat5*$^{-/-}$ cultured hepatocytes was impaired. In HEK293 cells, signaling by ectopically expressed glucagon receptor was increased by Mgat5 expression and GlcNAc supplementation to UDP-GlcNAc, the donor substrate shared by Mgat branching enzymes. The mobility of glucagon receptor in primary hepatocytes was reduced by galectin-9 binding, and the strength of the interaction was dependent on Mgat5 and UDP-GlcNAc levels. Finally, oral GlcNAc supplementation rescued the glucagon response in *Mgat5*$^{-/-}$hepatocytes and mice, as well as glycolytic metabolites and UDP-GlcNAc levels in liver. Our results reveal that the hexosamine biosynthesis pathway and GlcNAc salvage contribute to glucose homeostasis, through N-glycan branching on glucagon receptor.

---

The major biological function of the pancreatic hormone glucagon is to counteract the glucose-lowering action of insulin and maintain blood glucose concentration during fasting (1,2). Indeed, the severe hyperglycemia and glucose intolerance that characterizes insulin-deficient mice is reversed by a deficiency in glucagon receptor (Gcgr), although the mice are more sensitive to prolonged fasting (3-6). These experiments appear to unmask more ancient levels of feedback regulation that underpin insulin and glucagon signaling. In *S. cerevisiae*, glucose perception and import are separate modules that interact through posttranslational modifications (PTMs) signaling to regulate metabolism and growth rates (7,8). Kinases and phosphatases mediate rapid allosteric regulation of enzymes, while protein N-glycosylation adapts cell surface receptors and transporters to extracellular conditions (9).

Biosynthesis of high-energy PTM substrates such as acetyl-CoA (10), and UDP-GlcNAc are key to nutrient sensing (11-15). Fructose-6P, glutamine and acetyl-CoA are pivotal substrates in multiple pathways including the hexosamine biosynthesis pathway (HBP) to UDP-GlcNAc (9,16). Both O-GlcNAcylation of transcription factors (17-19), and N-glycosylation of membrane proteins have been identified as effectors of UDP-GlcNAc in glucose homeostasis (12,20). However, these effector pathways remain poorly understood (21).

Membrane receptors and solute transporters are cotranslationally modified in rough endoplasmic reticulum (ER) by oligosaccharyltransferase, which transfers the N-glycan from $Glc_3Man_9GlcNAc_2$-pp-dolichol to Asn at NXS/T(X≠P) sites. N-glycosylation is found in all domains of life (22,23), and has an ancient function that promotes protein folding in the endoplasmic reticulum. Protein synthesis and chaparone-assisted homeostasis consumes a large portion of cellular resources, and under stress conditions, reduced biosynthesis of $Glc_3Man_9GlcNAc_2$-pp-dolichol activates the unfolded protein response, thus a metabolic mechanism of stress tolerance (24).

With metazoan evolution, the ER N-glycan modification became a platform for remodeling in the Golgi, and additional functionality at the cell surface. The N-glycans are trimmed and rebuilt beginning with the branching N-acetyl-glucosaminyltransferases, encoded by the *Mgat-1, Mgat-2, Mgat-4a/b/c* and *Mgat-5* genes (25) (Figure 1A). The branching enzymes form a linear pathway and require the donor substrate UDP-GlcNAc. The GlcNAc branches are extended with galactose, poly-N-acetyllactosamine, fucose and sialic acid, generating sequences recognized by galectins, C-type lectins and siglecs at the cell surface. Galectin binding to Galβ1-4GlcNAcβ, a common sequence of N-glycan branches of membrane proteins, forms multivalent complexes, which results in a highly dynamic and heterogeneous lattice at the cell surface. Strong selective pressures on Golgi remodeling and its substrates during vertebrate evolution (26), have resulted in a layer of HBP-sensitive regulation for membrane receptors and solute transporters (12).

Glucose transporters (Glut) are dependent on N-glycan branching as reported forGlut2 in β-cells (20), Glut1 in tumor cells (27), and Glut4 (12,28). The *Mgat4a*$^{-/-}$ mice display suppressed secretion of insulin in response to glucose due to a failure to retain Glut2 at the surface ofβ-cells(20). The Mgat4a-branched N-glycan on Glut2 binds to galectin-9, which slows mobility at the cell surface and loss to endocytosis, thus increasing the transport of glucose, and thereby insulin secretion. While *Mgat4a*$^{-/-}$ mice display

hypoinsulinemia and excess weight-gain on a high-fat diet, *Mgat5*$^{-/-}$ mice are resistant to weight gain and display hyperglucagonemia (29), suggesting either a gain of function in glucagon secretion and/or loss of function in hepatic glucagon receptor (Gcgr). Mice lacking Gcgr display resistance to obesity on a high-fat diet with elevated circulating glucagon (30,31). Receptor deficiencies often result inelevated levels of the cognate ligand due to feedback up-regulation of ligand production or secretion, and/or failure to internalize and clear the ligand in the absence of receptor. Therefore, we hypothesized that the Gcgr may be regulated by Mgat5-dependent N-glycan branching in an HBP-dependent manner.

The Gcgr is a member of the class B G-protein coupled receptor superfamily (32) and activation results in the replacement of GDP with GTP bound to the $G_s\alpha$ subunit of the α/β/γ heterotrimeric complex. The GTP-bound $G_s\alpha$ activates adenylyl cyclase, and cAMP stimulates PKA, glycogen phosphorylase kinase and glycogen phosphorylase leading to hepatic glycogenolysis and gluconeogenesis (33). Inhibition of glucagon action attenuates hyperglycemia in experimental models and in subjects with type 2 diabetes (34). Here we report that *Mgat5*$^{-/-}$ mice and primary hepatocytes are hyposensitive to glucagon. The Mgat5-branched N-glycans on Gcgr increases receptor binding to galectin-9, which slow mobility and increases responsiveness to glucagon. GlcNAc supplementation increases UDP-GlcNAc flux to N-glycan branching in primary hepatocytes, and GlcNAc supplementation to *Mgat5*$^{-/-}$mice restored the glycemic response to glucagon. Our findings reveal a role for HBP and N-glycan branching on Gcgr as a positive regulator of glucagon responsiveness.

## EXPERIMENTAL PROCEDURE

**Mice-** Age and sex-matched littermates on the C57BL/6 background were used in all the experiments. The *Mgat5*$^{-/-}$ mutation was described previously (35), and made isogenic on C57BL6 by 15 generations of back-crosses. The *Mgat5*$^{-/-}$ hypoglycaemia phenotype has been validated on both 129/sv and C56BL6 backgrounds (29). Mice were maintained on a standard rodent chow (Teklad rodent diet, 18% protein, 6% fat, #2018) with a normal 12 h light/12 h dark cycle. In some experiments, mice were on low fat diet (Teklad rodent diet, 19% protein, 4% fat, #8604) or high fat diet (Teklad rodent diet, 19% protein, 9.8% fat, #2019) with or without GlcNAc (0.5 mg/ml) in the drinking water as indicated. Experiments were done according to protocols and guidelines approved by the Toronto Centre for Phenogenomics (TCP) animal care committee.

**Glucose tolerance, glucagon challenge, or insulin tolerance test-** For glucose tolerance tests (IPGTT), mice were fasted for 16 h before intraperitoneal injection of 0.01 ml/g body weight of a glucose solution containing 150 mg/ml. For oral glucose tolerance test (OGTT), a glucose solution was administered by oral gavage. Blood samples were drawn via the tail vain, and glucose measured using a Glucometer Elite blood glucose meter (Bayer, Toronto, ON). For the glucagon challenge test (GC), or insulin tolerance test (ITT), mice were fasted for 5h and injected intraperitoneally with a glucagon solution of 1.6 μg/ml (0.01 ml/g body weight) (16 μg/kg) or 0.75 U/kg of human insulin, respectively. Plasma glucagon and insulin were measured using a Mouse Endocrine LINCOplex kit (Linco Research) following the manufacturer's protocol. To measure the glycogen content in liver, 20-50 mg of tissue was acid hydrolyzed in 2 M HCl at 95°C for

2 h and neutralized using 2 M NaOH. The liberated glucose was assayed spectrophotometrically using the Glucose-Reagent (hexokinase method) (Amresco, OH) following the manufacturer's protocol.

**Primary hepatocytes and glucose secretion-** Murine hepatocytes were isolated as previously described (36), seededin6 well plates at4 x $10^5$ cells/well in Williams E media, containing 5% FBS and 0.7 mM insulin for 3 h to allow attachment. The cells were washed with PBS and DME media without glucose and phenol red. Cells were stimulated with 20 nM of glucagon and media was collected after 30 min, 1 h, 3 h, and 6 h, and stored at -20°C. To determine the residual glucose concentration in the cells, 2 N ice-cold HCL was added to cells, and lysates were incubated for 2h at 95°C followed by neutralization using 2 N NaOH. Glucose concentration in media and lysates were measured using the Glucose Reagent (hexokinase method) (Amresco, Solo, OH).

**LC-MS/MS analysis of metabolites-** Frozen liver tissue (80-100 mg) was crushed using the CellCrusher$^{TM}$ Cryogenic Tissue Pulveriser under liquid nitrogen, and 1 ml of ice-cold solution of (40% acetonitrile, 40% methanol, and 20% water) was added for metabolite extraction. For cells grown in cell culture plates, metabolites were extracted by adding 1 ml of ice-cold extraction solution(40% acetonitrile, 40% methanol, and 20% water) to the plate, scraping the cells and collecting in 1.5ml vials (16). Samples were separated twice on a reversed phase HPLC column Inertsil ODS-3, 4.6 mm internal diameter, 150 mm length, and 3 µM particle size (Dionex Corporation, CA) for MS analysis in positive and negative modes. The eluted metabolites were analyzed at the optimum polarity in MRM mode on electrospray ionization (ESI) triple-quadrupole mass spectrometer (ABSciex4000Qtrap, Toronto, ON, Canada) as previously described (16).

**Glucagon signaling-** Primary hepatocytes seeded on 24 well plates at a density of 1x$10^5$cells/ml were cultured in Williams E medium without FBS for 16 h, then supplemented with 100 µmol/l isomethyl butyl xanthine containing 0, 0.01, 0.1, 1.0, 10, 100 or 1000 nM glucagon and incubated for 10 min at 37°C. The reaction was stopped with ice-cold ethanol, and cAMP was measured by radioimmunoassay kit or targeted mass spectrometry using electrospray ionization triple-quadrupole ABSciex4000Qtrap (LC-MS/MS).

HEK293 Flp-In-TREx cells were purchased from Invitrogen and maintained in DMEM (Sigma) supplemented with 10% fetal bovine serum (FBS), 2 mM Gln, penicillin/streptomycin, and 3 ug/mL Blastocidin and 100 ug/mL Zeocin. Human *Mgat5* cDNA wes FLAG-tagged at the N-terminus, and cloned into the pcDNA5/FRT/TO expression vector. The plasmid was integrated into the genome at a pre-integrated FRT recombination site, by co-transfection with Flp recombinase encoding POG44 plasmid, using Lipofectamine (Invitrogen) and OptiMEM media lacking FBS or antibiotics. Following selection in 200 ug/mL of Hygromycin, clones displayed 5-10 fold increase in Mgat5 enzyme activity when induced by 1 ug/mL tetracycline for 24h. For Gcgr signalling in HEK293 Flp-In-TREx cells were transfected with 1 µg of Gcgr plasmid DNA using Lipofectamine 2000 reagent (Invitrogen, Carlsbad, CA). The next day cells were incubated with media containing 1 µg/ml tetracycline and GlcNAc as indicated for 24 h. Cells were stimulated with glucagon as described, and cAMP was measured by targeted LC/MS-MS.

**Membrane preparation and competitive glucagon binding assay-** Plasma membranes were prepared from primary hepatocytes using a cell surface isolation kit (Pierce, Rockford, IL)

following the manufacturer's protocol. Plasma membrane preparation were analysed via western blot, and the ImageJ software was used to quantify signal intensity (37). For liver membrane preparations, approximately 2 g of liver tissue were homogenized in 15 ml of 0.32 M sucrose solution at 4°C using a teflon tissue grind tube SZ23 (Kontess Class Co., Vinland, NJ). Homogenates were centrifuged at 4°C for 10 min at 600 x g. The supernatant was transferred to an ultra-clear ultracentrifuge tube (25 x 89 mm, Beckmann Coulter, Inc., Brea, CA) and underlayed with 15 ml of a 41% sucrose solution, followed by centrifugation at 100 000 x g for 17 h at 4°C. Membranes were collected at the interface, washed twice with 15 ml of 50 mM Tris/HCl buffer pH 7.5, and protein concentration was measured using the Pierce BCA protein assay kit (Thermo scientific, Rockford, IL).

$^{125}$I labeled glucagon (50,000 cpm, Perkin Elmer) was diluted in 100µl buffer. 40µg of membrane preparation was dissolved in 200µl buffer **(**25 mM HEPES, 2.5mM $CaCl_2$, 1.0mM $MgSO_4$, 0.05% bacitracin, 2% BSA, 0.003% Tween 20). Tracer, membrane preparation and 200 µl of glucagon solution at a final concentration from $10^{-12}$ to $10^{-6}$ M were incubated for 1 h at room temperature. To measure non-specific binding, 1 mM non-labeled glucagon was added to control samples. Binding reaction was stopped with 3 ml of buffer and immediately filtered through glass microfiber filters (Whatman GF/B). Filters were washed twice and radioactivity measured in a γ-scintillation counter. Experiments were carried out in duplicate with four independent liver membrane preparations. Insulin binding was measured with $^{125}$I labeled insulin (50,000 cpm Perkin Elmer) in 100 µl buffer incubated with 40µg of membrane preparation (200µl).

**Expression vectors-** Mouse Gcgr (NCBI clone NM_008101.2) was subcloned via EcoRI and HindIII restriction sites into a pcDNA3 (-) vector (Invitrogen, Carlsbad, CA). An internal Flag-tag (DYKDDDK) followed by a linker sequence containing four glycine residues were inserted at the N-terminus of the Gcgr after the putative cleavage signal site at amino acid 27 using a double joint PCR strategy (38). To generate a construct with an internal GFP-tag or FLAG-tag the same double joint PCR strategy was applied. GFP-Gcgr was subcloned into pEGFP-C1 vector with restriction enzymes AgeI and EcoRI. The glycosylation site mutants of Gcgr (ie. N47Q, N60Q, N75Q, N79Q, N118Q) were generated using site-directed mutagenesis. Mouse galectin-9 coding sequence (NCBI clone NM_001159301.1) was subcloned via Xho and EcoRI into pERFP-C1 vector (Clontech, Mountain view, CA).

**Western Blotting and immunoprecipitation-** Endogenous Gcgr was detected with ST-18 antibody (39). For chemical cross-linking to detectcell surface galectin and Gcgr, hepatocytes transfected with RFP-galectin-9 overnight were treated with 0.1 mg/ml 3,3´-Dithiobis (sulfosuccinimidylpropionate) (DTSSP) for 15 min at room temperature. Complexes were pulled down with rabbit anti-RFP antibody and protein G Sepharose beads (GE Healthcare). For detection of Flag-Gcgr the anti-Flag antibody M2 (Sigma-Aldrich) was used.

For L-PHA lectin binding, cells in 96 well plates were fixed for 15min with 4% paraformaldehyde, washed with PBS, and incubated for 1h at 20°Cin 50µL PBS containing 1/5000 of Hoechst 33342 and 2ug/ml Alexa Fluor-488 conjugated Leucoagglutinin (L-PHA) (Invitrogen, Carlsbad, CA). After washing with PBS, cell staining was quantified by IN Cell Analyzer 1000 automated fluorescence imaging.

**FRAP analyses-** Primary hepatocytes were seeded on 35 mm glass bottom culture dishes and transfected with 1 μg GFP-Gcgr and/or RFP-galectin-9 using Lipofectamine 2000 reagent. The next morning FRAP analyses was performed at RT on a confocal FV1000 Olympus microscope, with 405 nm laser at full power in a circular region of interest with 50-pixel diameter. Cells were incubated with 30 mM lactose for 4 h prior to the FRAP experiment, or overnight with 100 μM castanospermine or 20 mM GlcNAc supplementation in Williams E media. Fluorescence during recovery was normalized to the pre-bleach intensity and data averaged for a minimum of four to five animals in independent experiments in which 6 to 10 cells were bleached.

**Statistical analyses-** Statistical significance was assessed by one-way or two-way ANOVA using Bonferroni's multiple comparison post-test and, where appropriate, by Student's t-test using GraphPad Prism 5 (GraphPad Software; San Diego, CA). A p value $< 0.05$ was considered to be statistically significant.

## RESULTS

***Hypoglycemia and impaired glucagon response in Mgat5$^{-/-}$ mice-*** To characterize the metabolic phenotype in *Mgat5*$^{+/+}$ and *Mgat5*$^{-/-}$ mice, blood glucose, glucagon and insulin levels were measured in 6 month old male mice. Significantly lower blood glucose was observed in *Mgat5*$^{-/-}$ mice, in both the fed state, and after 5 h and 16 h of fasting, despite a 2-fold increase in serum glucagon levels and a 4-fold reduction in insulin levels in *Mgat5*$^{-/-}$ mice (Figure 1B-D). To examine the dynamics of glucose regulation in vivo, intraperitoneal (IPGTT) and oral (OGTT) glucose tolerance tests were performed in 8 to 12 month old male and female mice. Consistent with the propensity for glucose intolerance to increase with age (40), older male C57BL6 *Mgat5*$^{+/+}$ mice exhibited a marked glucose intolerance (Figure 1E,F) and impaired insulin sensitivity (Figure 1G). However, the *Mgat5*$^{-/-}$ male mice displayed remarkably improved glucose tolerance in both IPGTT and OGTT. In the insulin tolerance test (ITT), blood glucose in *Mgat5*$^{-/-}$ decreased to levels below those observed in wild type mice, and normalization was delayed, indicating a robust response to insulin but a deficient counter regulatory response to hypoglycemia (Figure 1G). Indeed, the *Mgat5*$^{-/-}$ male mice displayed an impaired response in the glucagon challenge (GC) test (Figure 1H). At 6 months, *Mgat5*$^{-/-}$ female mice were comparable to wild type, but at 12 months of age also displayed the phenotype of reduced sensitivity to glucagon and improved glucose tolerance (Figure 2A-E).

As with human aging (41), older *Mgat5*$^{+/+}$ mice exhibited increasing glucose intolerance, which is an important consideration in the natural history of type 2 diabetes. Therefore IPGTT was performed in older mice to determine when mutant and wild type phenotypes could be distinguished. The mutant phenotype was more severe in older female mice (Figure 2A-E). Glucose tolerance was similar in *Mgat5*$^{+/+}$ and *Mgat5*$^{-/-}$ mice at 3 and 4 months of age, whereas by 6 months *Mgat5*$^{-/-}$ mice displayed significantly improved glucose tolerance relative to *Mgat5*$^{+/+}$ littermates (Figure 3A-D). In the ITT, blood glucose levels in *Mgat5*$^{-/-}$ mice drop below that of controls, although the relative change from basal levels was similar, reflecting a near normal insulin response (Figure 3E). Importantly, at 6 months of age *Mgat5*$^{-/-}$ mice displayed a significantly diminished glycemic response to glucagon (Figure 3F).

The *Mgat5*$^{-/-}$ defect in glucagon signaling was predicted to qualitatively phenocopy *Gcgr*$^{-/-}$ mice. Indeed, liver

glycogen content in *Mgat5*$^{-/-}$ mice was increased in the fed state compared to wild type controls (Figure 4A). Metabolite profiling using targeted LC-MS/MS revealed a significant 2-6 fold increase in hepatic amino acid content in *Mgat5*$^{-/-}$ liver (Figure 4B). The glycogenic amino acids Ala, Thr, Gly, Arg, Ser and Asn were most affected, similar to the metabolic profiles described in *Gcgr*$^{-/-}$ mice (42). The levels of glycolytic intermediates were reduced, consistent with reduced glucose availability and gluconeogenesis (Figure 4C). HBP intermediates were also reduced, including UDP-GlcNAc, the donor substrate for N-glycan branching enzymes (Figure 4D).

***Gcgr in liver is modified by Mgat5-*** To assess the contribution of Mgat5 activity to N-glycan structures on Gcgr, hepatic lysates were analyzed by gel electrophoresis and Western blotting. Gcgr from *Mgat5*$^{-/-}$ liver migrated at ~70 kDa compared to ~75 kDa in *Mgat5*$^{+/+}$ extracts, consistent with the less branched N-glycans due to an absence of the Mgat5 branch and its extension (Figure 5A). After removal of N-glycans by PNGase F digestion, *Mgat5*$^{+/+}$ and *Mgat5*$^{-/-}$ Gcgr migrated at an identical molecular weight of ~50 kDa, confirming that the N-glycans were responsible for the difference observed in apparent molecular weight of Gcgr. Total Gcgr protein levels were similar in *Mgat5*$^{+/+}$ and *Mgat5*$^{-/-}$ livers by Western blotting, suggesting no differences in Gcgr protein expression. Flag-Gcgr expressed in Mgat5 and Mgat1 mutant CHO cell also indicated that Gcgr is a substrate of Mgat5, and the additional mass is distributed across multiple N-glycan sites (Figure 5B).

N-glycan multiplicity (NXS/T sites per glycoprotein) increases affinity for lectins with functional consequences, as reported for ER chaperones calnexin and calreticulin, and the galectins at the cell surface (12,43). To determine whether each of the five NXS/T sites in murine Gcgr are occupied by N-glycans, the sites were individually mutated from N to Q. Flag-Gcgr mutants and wild type Flag-Gcgr were transiently expressed in HEK293 cells and protein lysates were analyzed via Western blotting. All N-glycosylation site mutants displayed a small reduction in molecular weight for the lower-molecular weight, pre-Golgi form of the glycoprotein, suggesting all five NXS/T sites carry N-glycans (Figure 5C). The Golgi modifications generate size heterogeneity and contribute to the higher molecular weight forms of the receptor. Removal of N-glycans with PNGase F treatment resulted in migration at the same molecular weight (~50 kDa) for wild type and single-site mutants. The wild type and single site N-glycosylation mutants (N47Q, N60Q, N75Q, N79Q, N118Q) expressed in HEK293 cells, displayed similar cAMP response under glucagon stimulation, suggesting that individually, sites were not essential for folding in the ER, or for receptor activation (Figure 5D). Therefore, N-glycan branching and functionality may be distributed over multiple sites.

***Gcgr signaling is impaired in Mgat5*$^{-/-}$ *hepatocytes-*** Next we compared Gcgr signaling and glucose production in primary hepatocytes from *Mgat5*$^{-/-}$ and *Mgat5*$^{+/+}$mice. *Mgat5*$^{-/-}$ hepatocytes were less sensitive to glucagon-induced activation of adenylyl cyclase, with a log$EC_{50}$ of 1.016 ± 0.206 nM compared to 0.475 ± and 33.61 ± 2.73 nM) (Figure 6A). Direct stimulation of adenylyl cyclase by forskolin treatment increased cAMP to similar levels in mutant and wild type hepatocytes, indicating that the *Mgat5*$^{-/-}$ deficiency is upstream of adenylyl cyclase (Figure 6B). Glucagon stimulated production and secretion of glucose was reduced in *Mgat5*$^{-/-}$ hepatocytes (Figure 6C), whereas intracellular levels were not reduced (Figure 6D). Glucose inside the cells during the initial 1h of glucagon treatment declined at a similar

rate, suggesting that secretion was not impaired in *Mgat5*$^{-/-}$ hepatocytes, but rather Gcgr-driven gluconeogenesis was reduced.

***Gcgr binds galectin-9-*** In tumor cells, the branching of N-glycans on EGF and TGF-β receptors drives affinity for galectins that restrict mobility at the cell surface and promote sensitivity to ligand (44). Therefore we first compared Gcgr expression at the cell surface in primary hepatocytes by chemical tagging of surface proteins with biotin, and affinity purification on streptavidin beads. Western blotting revealed similar amounts of biotinylated-Gcgr on *Mgat5*$^{+/+}$ and *Mgat5*$^{-/-}$ hepatocytes (Figure 7A,B). However, Gcgr in liver membrane preparations from *Mgat5*$^{-/-}$ exhibited reduced affinity in a competitive glucagon binding assay (Figure 7C). Maximal binding was reduced by 18% and affinity for glucagon was also reduced from 1.17 x$10^{-10}$ M in *Mgat5*$^{+/+}$ to 1.33 x$10^{-9}$ Min*Mgat5*$^{-/}$. Insulin binding was also measured and found to be similar in *Mgat5*$^{+/+}$ and *Mgat5*$^{-/-}$ membrane preparations (Figure 7D).

The galectin-9 gene is more highly expressed in liver than other members of the galectin family, making it a likely candidate for interaction with Gcgr (45) (Figure 7E). Therefore, RFP-galectin-9 was expressed in primary hepatocytes, followed by cross-linking and protein complexes were captured on anti-RFP antibody-coated beads. Endogenous Gcgr was present in the RFP-galectin-9 captured glycoproteins, and to a greater extent in *Mgat5*$^{+/+}$ than *Mgat5*$^{-/-}$ (Figure 7F). Pretreatment of the hepatocytes with lactose, a competitive inhibitor of galectin binding, reduced Gcgr–RFP-galectin-9 association confirming that the carbohydrate-reactive domain of galectin-9 is required for this interaction.

***Gcgr dynamics are dependent on N-glycan branching, HBP and galectin-9-*** Branched N-glycans on glycoproteins are the major ligands for galectin binding at the cell surface (46). Fluorescence recovery after photobleaching (FRAP) has previously been used to measure the interaction of EGF receptor with galectin-3 on tumor cells (47). The strength of the interaction is proportional to the half-time of recovery after photobleaching ($t_{1/2}$). FRAP analyses were performed on GFP-Gcgr expressed in primary hepatocytes from *Mgat5*$^{-/-}$ and *Mgat5*$^{+/+}$ mice (Figure 8 A,B). GFP-Gcgr showed similar maximal recovery after photobleaching, but recovery was faster ie. lower $t_{1/2}$) in *Mgat5*$^{-/-}$ cells, indicating greater mobility compared to *Mgat5*$^{+/+}$ (Figure 8C). Treatment of cells with lactose, a competitive inhibitor of galectin-binding, reduced $t_{1/2}$ in *Mgat5*$^{+/+}$ cells (Figure 8D,E). Similarly, inhibition of N-glycan branching with the α-glucosidase I/II inhibitor castanospermine decreased $t_{1/2}$in *Mgat5*$^{+/+}$cells. Lactose and castanospermine did not further reduce $t_{1/2}$ in the *Mgat5*$^{-/-}$ cells. Co-expression of galectin-9 with GFP-Gcgr increased $t_{1/2}$, indicting decreased receptor mobility by ~2 fold in both *Mgat5*$^{+/+}$ and *Mgat5*$^{-/-}$ hepatocytes relative to their respective controls (Figure 8D,E). This is consistent with galectin-9 binding to Gcgr, and presumably other glycoproteins at the cell surface with graded affinities proportional to branching.

In immortalized cells and primary T cells, flux through the HBP and/or salvage of GlcNAc have been shown to increase intracellular UDP-GlcNAc levels, N-glycan branching and receptor retention at the cell surface (14,48). To explore this possibility for Gcgr, primary hepatocytes were supplemented with GlcNAc for 16h prior to FRAP analysis. GlcNAc increased receptor $t_{1/2}$ for both *Mgat5*$^{-/-}$ and *Mgat5*$^{+/+}$ cells, and hence decreased receptor mobility (Figure 8D,E). Castanospermine treatment completely blocked the effects of GlcNAc supplementation on GFP-Gcgr mobility,

confirming that GlcNAc strengthens galectin-glycoprotein interactions by enhancing N-glycan branching. The combination of galectin-9 expression and GlcNAc supplementation did not show an additive effect in *Mgat5*$^{+/+}$ but a small enhancement over galectin-9 alone was observed for *Mgat5*$^{-/-}$ cells (Figure 8D,E), consistent with the expectation that N-glycan branching is more limiting in the mutant.

GlcNAc also enhanced glucagon-dependent stimulation of adenylyl cyclase in primary hepatocytes from *Mgat5*$^{-/-}$ mice but with less effect in *Mgat5*$^{+/+}$ (Figure 9A). The *Mgat5*-deficiency also results in increased salvage into GlcNAc-P (12), possibly reflecting feedback in the hypoglycemic state that normally increases HBP flux to N-glycan branching and enhanced Gcgr sensitivity (Figure 9B). UDP-GlcNAc was increased by 5-7 fold in both mutant and wild type cells (Figure 9B). GlcNAc ineffectiveness on Gcgr signaling in *Mgat5*$^{+/+}$hepatocytes suggests negative feedback that normally opposes hyper-responsiveness to Gcgr.

To reconstruct the molecular interactions between HBP and Mgat5 in an independent cell line, HEK293 cells with a tetracycline (tet)-inducible Mgat5 transgene were transiently transfected with a Gcgr expression vector. In these cells, glucagon-dependent stimulation of adenylyl cyclase was enhanced by GlcNAc supplementation alone, and tet-induced Mgat5 had an additive effect (Figure 9C). GlcNAc supplementation increased intracellular UDP-GlcNAc as observed in hepatocytes, and increased Mgat5-dependent branching in a synergistic manner detected via L-PHA staining of the cell surface (Figure 9D,E). Induced Mgat5 expression alone did not increase Gcgr activity, suggesting that UDP-GlcNAc supply is a limiting factor for the branching pathway, and acts cooperatively with Mgat5. This relationship is consistent with results in primary hepatocytes (Figure 9C-E).

***GlcNAc supplementation rescues sensitivity to glucagon in Mgat5$^{-/-}$ mice-*** GlcNAc supplementation in the drinking water of mice increases N-glycan branching on T cell receptors and regulates sensitivity to autoimmune antigens (49). Therefore, we tested whether GlcNAc in the drinking water (0.5 mg/ml) could increase Gcgr sensitivity. This dose of GlcNAc was <1% of carbohydrate equivalents in the mouse diet. Moreover, catabolism of GlcNAc-6-P by deacetylase activity is very low or absent in mammalian cells (14). Thus salvaged GlcNAc contributes to the UPD-GlcNAc pool and down-stream effector pathways, rather than to the glucose pool (16). Since *Mgat5*$^{-/-}$ mice are hypoglycemic and resistant to weight gain on a high fat diet (29), we reasoned that rescue by GlcNAc may be more robust on a calorie-enriched diet. Mice were maintained on GlcNAc from weaning to 8 months of age, when glucagon challenge (GC) and glucose tolerance (IPGTT) were measured. GlcNAc supplementation resulted in a significantly improved response to glucagon in *Mgat5*$^{-/-}$ mice, but little effect in *Mgat5*$^{+/+}$ mice (Figure 10A,B). GlcNAc did not alter IPGTT in either genotype, indicating that supplementation did not cause insulin resistance (Figure 10C,D). UDP-GlcNAc and GlcNAc-P levels were increased in *Mgat5*$^{-/-}$ liver, consistent with enhanced HBP-dependent positive feedback in mutant mice (Figure 10E,F). The same trend in *Mgat5*$^{+/+}$ did not reach significance. Hepatic glucose-P and fructose-P levels were increased in *Mgat5*$^{-/-}$ mice by GlcNAc, which is a reversal of the *Mgat5*$^{-/-}$ mutant phenotype (Figure 10F and 4D).

## DISCUSSION

In this report, we tested the hypothesis that Gcgr sensitivity is dependent on modification by Mgat5 and more broadly, the N-glycan branching pathway. We demonstrate that *Mgat5*$^{-/-}$ mice are hypoglycemic, display improved glucose tolerance, and decreased sensitivity to glucagon. HBP and glycolytic metabolites were decreased, while glycogen storage and free amino acids were increased in *Mgat5*$^{-/-}$ livers; a regulatory imbalance similar to that reported for *Gcgr*$^{-/-}$ mice (42). The *Mgat5*$^{-/-}$ mice displayed a remarkably similar glucoregulatory phenotype to mice deficient in either glucagon processing or Gcgr signaling (3,30,31). Furthermore, experiments with primary hepatocytes confirmed that glucagon-dependent cAMP signaling is impaired and gluconeogenesis reduced by the Mgat5 deficiency. Reduced hepatic catabolism of amino acids and glycogen may also contribute to lower glucose production and systemic hypoglycemia. The $EC_{50}$ for glucagon-dependent activation of adenylyl cylase was increased ~4 fold in *Mgat5*$^{-/-}$primary cells. Plasma membrane levels of Gcgr were similar, but glucagon binding sites were reduced by 18% and affinity was reduced~10 fold in *Mgat5*$^{-/-}$membrane preparations. GlcNAc supplementation, Mgat5 and N-glycan branching were shown to promote Gcgr association with galectin-9, which slows receptor mobility and enhances sensitivity to glucagon in primary hepatocytes. Finally, GlcNAc supplementation in the drinking water rescued glucagon sensitivity in *Mgat5*$^{-/-}$ mice, concordant with the GlcNAc rescue of Gcgr signaling and dynamics in cultured primary hepatocytes. Importantly, GlcNAc supplementation did not alter glucose tolerance in either wild type or mutant mice, suggesting that insulin action was not impaired by GlcNAc. The results suggest a model for metabolic feedback through HBP and N-glycan branching in the regulation of Gcgr (Figure 11).

Experimental deletion of the N-glycosylation sites in Gcgr, GIP and GLP-1 receptors blocks protein expression at the cell surface (50,51), which is likely due to receptor instability or misfolding. The removal of NXS/T(X≠P) sites is a blunt instrument that precludes the analysis of Golgi N-glycan remodeling pathways. The present study is the first to reveal that N-glycan remodeling is an effector down-stream of HBP that regulates responsiveness of a critical receptor in glucose homeostasis. Individual sites in Gcgr were not critical, as mutation of each site did not disrupt receptor activities measured in HEK293 cells. This suggests that functionality of N-glycan branching may be cumulative and distributed over the five sites in Gcgr.

We show that galectin-9 binds to Gcgr and slows receptor mobility, with a dependency on Mgat5 activity and UDP-GlcNAc supply to the N-glycan branching pathway. Galectin-9 binding promotes cross-linking of glycoproteins, and may facilitate Gcgr dimerization(52),or association with other glycoproteins. Dimerization of the GLP-1R promotes coupling with G protein-coupled receptors and sensitivity to ligand (53). All nine mammalian adenylyl cyclases share conserved *N*-glycosylation sites in extracellular loops five and six (54). N-glycosylation of adenylyl cyclase 8 is required to target the enzyme into lipid raft domains (55) and Golgi modifications may play a role in efficient coupling of this adenylyl cylase with Gcgr. The receptor activity-modifying protein-2 (RAMP-2) is another transmembrane glycoprotein shown to be associated with Gcgr (56). It is likely that galectin-9 slows down not only the mobility of Gcgr, but also other glycoproteins and regulates signaling efficiency. Thus, galectin-9 binding to

branched N-glycan on Gcgr may slow mobility, and thereby enhance interactions with other regulatory glycoproteins. It is also possible that branched N-glycans interact within the receptor fold to enhance dimerization and/or affinity for ligand (57).

In the absence of Mgat5, compensating amounts of N-acetyllactosamine (Galβ1-4GlcNAcβ) branches can be made by Mgat1, Mgat2 and Mgat4 when supplied with GlcNAc (12,58), which is converted into UDP-GlcNAc. Indeed, glucagon sensitivity in *Mgat5*$^{-/-}$ mice was rescued by GlcNAc supplied in the drinking water. GlcNAc supplementation at 0.5 mg/ml increased liver HBP metabolites in *Mgat5*$^{-/-}$mice, rescued Gcgr membrane dynamics as well as cAMP signaling in cultured primary hepatocytes. The interaction between Mgat5, UDP-GlcNAc, Gcgr and cAMP signaling was engineered into HEK293 cells, and found to be very similar to primary hepatocytes. Gcgr sensitivity to glucagon was highest when Mgat5 was induced in the presence of GlcNAc supplementation. Mgat5 has a low affinity for UDP-GlcNAc (Km ~10 mM) relative to Mgat1, Mgat2 and Mgat4. Therefore, Mgat5 activity is highly dependent on UDP-GlcNAc concentration and enzyme levels. Conversely, expression of Mgat5 is relatively low in liver compared to intestine and brain (59), suggesting that regulation of branching may be highly dependent on HBP and central metabolites. *Mgat5* gene expression is stimulated by hepatic stress and growth factor-dependent activation of Ets transcription factors (60,61). In β-cells, Mgat4a gene expression is inhibited by the Foxa2 transcription factor under replete conditions (62). Hepatic Foxa2 is activated down-stream of glucagon signaling (fasting), and inhibited by insulin-Pi3k-Akt signaling (63). Additional studies are needed to map interactions between the expression of the Mgat genes and metabolite sensing both β-cells and hepatocytes.

Transgenic mice overexpressing the HBP enzyme, glutamine:fructose-6-phosphate amidotransferase (GFAT) in liver display obesity, glucose intolerance and insulin resistance after 8 months of age (64). Here we have extended these observations by identifying the Golgi N-glycan branching pathway as an effector down-stream of HBP that adapts hepatocyte responsiveness to glucagon. In addition to Gcgr, many other glycoproteins are known to be substrates for Mgat5-modification (65) and may contribute to glucose regulation. For example, TGF-β receptor II is up-regulated at the cell surface by HBP and Mgat5 in cultured cells (12,44). TGF-β/Smad3 signaling regulates glucose homeostasis, and Smad3$^{-/-}$ mice have a phenotype similar to that of *Mgat5*$^{-/-}$ (66). As discussed earlier, GLUT-1, -2 and -4 glucose transporters are up-regulated at the cell surface by N-glycan branching (12,20,27,28). Herein we have focused on Gcgr, as the action of glucagon is critically importance for the development of hyperglycemia and insulin resistance (1,2). Hence, selective reduction of Mgat5 activity or HBP in the liver may represent a novel approach for suppression of glucagon action and restoration of euglycemia in the setting of type 2 diabetes.

## REFERENCES


1. Ali, S., and Drucker, D. J. (2009) Benefits and limitations of reducing glucagon action for the treatment of type 2 diabetes. *Am J Physiol Endocrinol Metab* **296**, E415-421
2. Unger, R. H., and Cherrington, A. D. (2012) Glucagonocentric restructuring of diabetes: a pathophysiologic and therapeutic makeover. *J Clin Invest* **122**, 4-12
3. Conarello, S. L., Jiang, G., Mu, J., Li, Z., Woods, J., Zycband, E., Ronan, J., Liu, F., Roy, R. S., Zhu, L., Charron, M. J., and Zhang, B. B. (2007) Glucagon receptor knockout mice are resistant to diet-induced obesity and streptozotocin-mediated beta cell loss and hyperglycaemia. *Diabetologia* **50**, 142-150
4. Lee, Y., Berglund, E. D., Wang, M. Y., Fu, X., Yu, X., Charron, M. J., Burgess, S. C., and Unger, R. H. (2012) Metabolic manifestations of insulin deficiency do not occur without glucagon action. *Proc Natl Acad Sci USA* **109**, 14972-14976
5. Hancock, A. S., Du, A., Liu, J., Miller, M., and May, C. L. (2010) Glucagon deficiency reduces hepatic glucose production and improves glucose tolerance in adult mice. *Mol Endocrinol* **24**, 1605-1614
6. Vuguin, P. M., Kedees, M. H., Cui, L., Guz, Y., Gelling, R. W., Nejathaim, M., Charron, M. J., and Teitelman, G. (2006) Ablation of the glucagon receptor gene increases fetal lethality and produces alterations in islet development and maturation. *Endocrinology* **147**, 3995-4006
7. Youk, H., and van Oudenaarden, A. (2009) Growth landscape formed by perception and import of glucose in yeast. *Nature* **462**, 875-879
8. Thevelein, J. M., and Voordeckers, K. (2009) Functioning and evolutionary significance of nutrient transceptors. *Mol Biol Evol* **26**, 2407-2414
9. Dennis, J. W., Nabi, I. R., and Demetriou, M. (2009) Metabolism, cell surface organization, and disease. *Cell* **139**, 1229-1241
10. Wellen, K. E., Hatzivassiliou, G., Sachdeva, U. M., Bui, T. V., Cross, J. R., and Thompson, C. B. (2009) ATP-citrate lyase links cellular metabolism to histone acetylation. *Science* **324**, 1076-1080
11. Cooksey, R. C., and McClain, D. A. (2002) Transgenic mice overexpressing the rate-limiting enzyme for hexosamine synthesis in skeletal muscle or adipose tissue exhibit total body insulin resistance. *Ann N Y Acad Sci* **967**, 102-111
12. Lau, K. S., Partridge, E. A., Grigorian, A., Silvescu, C. I., Reinhold, V. N., Demetriou, M., and Dennis, J. W. (2007) Complex N-glycan number and degree of branching cooperate to regulate cell proliferation and differentiation. *Cell* **129**, 123-134
13. Metallo, C. M., and Vander Heiden, M. G. (2010) Metabolism strikes back: metabolic flux regulates cell signaling. *Genes Dev* **24**, 2717-2722
14. Wellen, K. E., Lu, C., Mancuso, A., Lemons, J. M., Ryczko, M., Dennis, J. W., Rabinowitz, J. D., Coller, H. A., and Thompson, C. B. (2010) The hexosamine biosynthetic pathway couples growth factor-induced glutamine uptake to glucose metabolism. *Genes Dev* **24**, 2784-2799
15. Denzel, M. S., Storm, N. J., Gutschmidt, A., Baddi, R., Hinze, Y., Jarosch, E., Sommer, T., Hoppe, T., and Antebi, A. (2014) Hexosamine pathway metabolites enhance protein quality control and prolong life. *Cell* **156**, 1167-1178
16. Abdel Rahman, A. M., Ryczko, M., Pawling, J., and Dennis, J. W. (2013) Probing the hexosamine biosynthetic pathway in human tumor cells by multitargeted tandem mass spectrometry. *ACS chemical biology* **8**, 2053-2062

17. Yang, X., Ongusaha, P. P., Miles, P. D., Havstad, J. C., Zhang, F., So, W. V., Kudlow, J. E., Michell, R. H., Olefsky, J. M., Field, S. J., and Evans, R. M. (2008) Phosphoinositide signalling links O-GlcNAc transferase to insulin resistance. *Nature* **451**, 964-969
18. Dentin, R., Hedrick, S., Xie, J., Yates, J., 3rd, and Montminy, M. (2008) Hepatic glucose sensing via the CREB coactivator CRTC2. *Science* **319**, 1402-1405
19. Slawson, C., Copeland, R. J., and Hart, G. W. (2010) O-GlcNAc signaling: a metabolic link between diabetes and cancer? *Trends Biochem Sci* **35**, 547-555
20. Ohtsubo, K., Takamatsu, S., Minowa, M. T., Yoshida, A., Takeuchi, M., and Marth, J. D. (2005) Dietary and genetic control of glucose transporter 2 glycosylation promotes insulin secretion in suppressing diabetes. *Cell* **123**, 1307-1321
21. Macauley, M. S., Shan, X., Yuzwa, S. A., Gloster, T. M., and Vocadlo, D. J. (2010) Elevation of Global O-GlcNAc in rodents using a selective O-GlcNAcase inhibitor does not cause insulin resistance or perturb glucohomeostasis. *Chemistry & Biology* **17**, 949-958
22. Banerjee, S., Vishwanath, P., Cui, J., Kelleher, D. J., Gilmore, R., Robbins, P. W., and Samuelson, J. (2007) The evolution of N-glycan-dependent endoplasmic reticulum quality control factors for glycoprotein folding and degradation. *Proc Natl Acad Sci USA* **104**, 11676-11681
23. Kowarik, M., Numao, S., Feldman, M. F., Schulz, B. L., Callewaert, N., Kiermaier, E., Catrein, I., and Aebi, M. (2006) N-linked glycosylation of folded proteins by the bacterial oligosaccharyltransferase. *Science* **314**, 1148-1150
24. Shang, J., Gao, N., Kaufman, R. J., Ron, D., Harding, H. P., and Lehrman, M. A. (2007) Translation attenuation by PERK balances ER glycoprotein synthesis with lipid-linked oligosaccharide flux. *J Cell Biol* **176**, 605-616
25. Dennis, J. W., Lau, K. S., Demetriou, M., and Nabi, I. R. (2009) Adaptive Regulation at the Cell Surface by N-Glycosylation. *Traffic* **11**, 1569-1578
26. Williams, R., Ma, X., Schott, R. K., Mohammad, N., Ho, C. Y., Li, C. F., Chang, B. S., Demetriou, M., and Dennis, J. W. (2014) Encoding asymmetry of the N-glycosylation motif facilitates glycoprotein evolution. *PLoS One* **9**, e86088
27. Kitagawa, T., Tsuruhara, Y., Hayashi, M., Endo, T., and Stanbridge, E. J. (1995) A tumor-associated glycosylation change in the glucose transporter GLUT1 controlled by tumor suppressor function in human cell hybrids. *J Cell Sci* **108 ( Pt 12)**, 3735-3743
28. Haga, Y., Ishii, K., and Suzuki, T. (2011) N-glycosylation is critical for the stability and intracellular trafficking of glucose transporter GLUT4. *J Biol Chem* **286**, 31320-31327
29. Cheung, P., Pawling, J., Partridge, E. A., Sukhu, B., Grynpas, M., and Dennis, J. W. (2007) Metabolic homeostasis and tissue renewal are dependent on beta1,6GlcNAc-branched N-glycans. *Glycobiology* **17**, 828-837
30. Gelling, R. W., Du, X. Q., Dichmann, D. S., Romer, J., Huang, H., Cui, L., Obici, S., Tang, B., Holst, J. J., Fledelius, C., Johansen, P. B., Rossetti, L., Jelicks, L. A., Serup, P., Nishimura, E., and Charron, M. J. (2003) Lower blood glucose, hyperglucagonemia, and pancreatic alpha cell hyperplasia in glucagon receptor knockout mice. *Proc Natl Acad Sci USA* **100**, 1438-1443
31. Sorensen, H., Winzell, M. S., Brand, C. L., Fosgerau, K., Gelling, R. W., Nishimura, E., and Ahren, B. (2006) Glucagon receptor knockout mice display increased insulin sensitivity and impaired beta-cell function. *Diabetes* **55**, 3463-3469

32. Mayo, K. E., Miller, L. J., Bataille, D., Dalle, S., Goke, B., Thorens, B., and Drucker, D. J. (2003) International Union of Pharmacology. XXXV. The glucagon receptor family. *Pharmacol Rev* **55**, 167-194
33. Jiang, G., and Zhang, B. B. (2003) Glucagon and regulation of glucose metabolism. *American journal of physiology. Endocrinol and Metabol* **284**, E671-678
34. Cho, Y. M., Merchant, C. E., and Kieffer, T. J. (2012) Targeting the glucagon receptor family for diabetes and obesity therapy. *Pharmacol Ther* **135**, 247-278
35. Granovsky, M., Fata, J., Pawling, J., Muller, W. J., Khokha, R., and Dennis, J. W. (2000) Suppression of tumor growth and metastasis in Mgat5-deficient mice. *Nature Medicine* **6**, 306-312
36. Flock, G., Baggio, L. L., Longuet, C., and Drucker, D. J. (2007) Incretin receptors for glucagon-like peptide 1 and glucose-dependent insulinotropic polypeptide are essential for the sustained metabolic actions of vildagliptin in mice. *Diabetes* **56**, 3006-3013
37. Schneider, C. A., Rasband, W. S., and Eliceiri, K. W. (2012) NIH Image to ImageJ: 25 years of image analysis. *Nature methods* **9**, 671-675
38. Yu, C. E., Devlin, B., Galloway, N., Loomis, E., and Schellenberg, G. D. (2004) ADLAPH: A molecular haplotyping method based on allele-discriminating long-range PCR. *Genomics* **84**, 600-612
39. Unson, C. G., Cypess, A. M., Wu, C. R., Goldsmith, P. K., Merrifield, R. B., and Sakmar, T. P. (1996) Antibodies against specific extracellular epitopes of the glucagon receptor block glucagon binding. *Proc Natl Acad Sci USA* **93**, 310-315
40. Goren, H. J., Kulkarni, R. N., and Kahn, C. R. (2004) Glucose homeostasis and tissue transcript content of insulin signaling intermediates in four inbred strains of mice: C57BL/6, C57BLKS/6, DBA/2, and 129X1. *Endocrinology* **145**, 3307-3323
41. Petersen, K. F., Befroy, D., Dufour, S., Dziura, J., Ariyan, C., Rothman, D. L., DiPietro, L., Cline, G. W., and Shulman, G. I. (2003) Mitochondrial dysfunction in the elderly: possible role in insulin resistance. *Science* **300**, 1140-1142
42. Yang, J., MacDougall, M. L., McDowell, M. T., Xi, L., Wei, R., Zavadoski, W. J., Molloy, M. P., Baker, J. D., Kuhn, M., Cabrera, O., and Treadway, J. L. (2011) Polyomic profiling reveals significant hepatic metabolic alterations in glucagon-receptor (GCGR) knockout mice: implications on anti-glucagon therapies for diabetes. *BMC genomics* **12**, 281
43. Deprez, P., Gautschi, M., and Helenius, A. (2005) More than one glycan is needed for ER glucosidase II to allow entry of glycoproteins into the calnexin/calreticulin cycle. *Molecular Cell* **19**, 183-195
44. Partridge, E. A., Le Roy, C., Di Guglielmo, G. M., Pawling, J., Cheung, P., Granovsky, M., Nabi, I. R., Wrana, J. L., and Dennis, J. W. (2004) Regulation of cytokine receptors by Golgi N-glycan processing and endocytosis. *Science* **306**, 120-124
45. Bishop, J. R., Foley, E., Lawrence, R., and Esko, J. D. (2010) Insulin-dependent diabetes mellitus in mice does not alter liver heparan sulfate. *J Biol Chem* **285**, 14658-14662
46. Patnaik, S. K., Potvin, B., Carlsson, S., Sturm, D., Leffler, H., and Stanley, P. (2006) Complex N-glycans are the major ligands for galectin-1, -3, and -8 on Chinese hamster ovary cells. *Glycobiology* **16**, 305-317
47. Lajoie, P., Partridge, E. A., Guay, G., Goetz, J. G., Pawling, J., Lagana, A., Joshi, B., Dennis, J. W., and Nabi, I. R. (2007) Plasma membrane domain organization regulates EGFR signaling in tumor cells. *J Cell Biol* **179**, 341-356

48. Grigorian, A., Lee, S.-U., Tian, W., Chen, I.-J., Gao, G., Mendelsohn, R., Dennis, J. W., and Demetriou, M. (2007) Control of T cell mediated autoimmunity by metabolite flux to N-glycan biosynthesis. *J Biol Chem* **282**, 20027-20035
49. Grigorian, A., Araujo, L., Naidu, N. N., Place, D., Choudhury, B., and Demetriou, M. (2011) N-acetylglucosamine inhibits T-helper 1 (Th1) / T-helper 17 (Th17) responses and treats experimental autoimmune encephalomyelitis. *J. Biol. Chem.* **286**, 40133-40141
50. Unson, C. G., Cypess, A. M., Kim, H. N., Goldsmith, P. K., Carruthers, C. J., Merrifield, R. B., and Sakmar, T. P. (1995) Characterization of deletion and truncation mutants of the rat glucagon receptor. Seven transmembrane segments are necessary for receptor transport to the plasma membrane and glucagon binding. *J Biol Chem* **270**, 27720-27727
51. Whitaker, G. M., Lynn, F. C., McIntosh, C. H., and Accili, E. A. (2012) Regulation of GIP and GLP1 receptor cell surface expression by N-glycosylation and receptor heteromerization. *PloS one* **7**, e32675
52. Schelshorn, D., Joly, F., Mutel, S., Hampe, C., Breton, B., Mutel, V., and Lutjens, R. (2012) Lateral allosterism in the glucagon receptor family: glucagon-like peptide 1 induces G-protein-coupled receptor heteromer formation. *Mol Pharmacol* **81**, 309-318
53. Harikumar, K. G., Wootten, D., Pinon, D. I., Koole, C., Ball, A. M., Furness, S. G., Graham, B., Dong, M., Christopoulos, A., Miller, L. J., and Sexton, P. M. (2012) Glucagon-like peptide-1 receptor dimerization differentially regulates agonist signaling but does not affect small molecule allostery. *Proc Natl Acad Sci USA* **109**, 18607-18612
54. Wu, G. C., Lai, H. L., Lin, Y. W., Chu, Y. T., and Chern, Y. (2001) N-glycosylation and residues Asn805 and Asn890 are involved in the functional properties of type VI adenylyl cyclase. *J Biol Chem* **276**, 35450-35457
55. Pagano, M., Clynes, M. A., Masada, N., Ciruela, A., Ayling, L. J., Wachten, S., and Cooper, D. M. (2009) Insights into the residence in lipid rafts of adenylyl cyclase AC8 and its regulation by capacitative calcium entry. *Am J Physiol Cell physiol* **296**, C607-619
56. Christopoulos, A., Christopoulos, G., Morfis, M., Udawela, M., Laburthe, M., Couvineau, A., Kuwasako, K., Tilakaratne, N., and Sexton, P. M. (2003) Novel receptor partners and function of receptor activity-modifying proteins. *J Biol Chem* **278**, 3293-3297
57. McElroy, C. A., Dohm, J. A., and Walsh, S. T. (2009) Structural and biophysical studies of the human IL-7/IL-7Ralpha complex. *Structure* **17**, 54-65
58. Dennis, J. W., and Brewer, C. F. (2013) Density-dependent lectin-glycan interactions as a paradigm for conditional regulation by posttranslational modifications. *Mol Cell Proteomics* **12**, 913-920
59. Campbell, R. M., Metzler, M., Granovsky, M., Dennis, J. W., and Marth, J. D. (1995) Complex asparagine-linked oligosaccharides in Mgat1-null embryos. *Glycobiology* **5**, 535-543
60. Buckhaults, P., Chen, L., Fregien, N., and Pierce, M. (1997) Transcriptional regulation of N-acetylglucosaminyltransferase V by the src Oncogene. *J Biol Chem.* **272**, 19575-19581
61. Kang, R., Saito, H., Ihara, Y., Miyoshi, E., Koyama, N., Sheng, Y., and Taniguchi, N. (1996) Transcriptional regulation of the N-acetylglucosaminyltranserase V gene in human bile duct carcinoma cells (HuCC-T1) is mediated by Ets-1. *J Biol Chem.* **271**, 26706-26712

62. Ohtsubo, K., Chen, M. Z., Olefsky, J. M., and Marth, J. D. (2011) Pathway to diabetes through attenuation of pancreatic beta cell glycosylation and glucose transport. *Nature Med.* **17**, 1067
63. von Meyenn, F., Porstmann, T., Gasser, E., Selevsek, N., Schmidt, A., Aebersold, R., and Stoffel, M. (2013) Glucagon-induced acetylation of Foxa2 regulates hepatic lipid metabolism. *Cell Metab* **17**, 436-447
64. Veerababu, G., Tang, J., Hoffman, R. T., Daniels, M. C., Hebert, L. F., Jr., Crook, E. D., Cooksey, R. C., and McClain, D. A. (2000) Overexpression of glutamine: fructose-6-phosphate amidotransferase in the liver of transgenic mice results in enhanced glycogen storage, hyperlipidemia, obesity, and impaired glucose tolerance. *Diabetes* **49**, 2070-2078
65. Abbott, K. L., Aoki, K., Lim, J. M., Porterfield, M., Johnson, R., O'Regan, R. M., Wells, L., Tiemeyer, M., and Pierce, M. (2008) Targeted glycoproteomic identification of biomarkers for human breast carcinoma. *J Proteome Res* **7**, 1470-1480
66. Yadav, H., Quijano, C., Kamaraju, A. K., Gavrilova, O., Malek, R., Chen, W., Zerfas, P., Zhigang, D., Wright, E. C., Stuelten, C., Sun, P., Lonning, S., Skarulis, M., Sumner, A. E., Finkel, T., and Rane, S. G. (2011) Protection from obesity and diabetes by blockade of TGF-beta/Smad3 signaling. *Cell Metab* **14**, 67-79

**ACKNOWLEDGEMENTS**

Research was supported by grants from the Ontario Research Fund (GL-2) and Canadian Institutes for Health Research MOP-79405 and MOP-62975, the Canada Research Chairs Program to JWD and DJD, the Canadian Institutes for Health Research MOP-93749 and MOP 123391 to DJD, the BBDC-Novo Nordisk Chair in Incretin Biologyto DJD, and Canadian Liver Foundation Graduate Studentship to MR. We thank Cecilia Unson for the ST-18 antibody and Cecile Boscher and Oliver Rocks for experiment advice.

**FIGURE LEGENDS**

**Figure 1**

**Glucose distribution in male *Mgat5*$^{+/+}$ and *Mgat5*$^{-/-}$ mice- (A)** Proteins produced in the secretory pathway are N-glycosylated in the ER, followed by remodelling of the N-glycans in the Golgi. The medial Golgi N-acetylglucosaminyltransferases I, II, VI and V (MGAT1, 2, 4, 5 genes) initiate the GlcNAc-branches sequentially. The trans-Golgi β1,4galactosyltransferase extend GlcNAc-branches forming ligands for galectins, where affinity is proportional to branching. **(B)** Serum glucose levels at 6 month in fed and fasted conditions. **(C)** Plasma glucagon and **(D)** plasma insulin levels measured in male mice fasted 5h and 16h (n=4 to 8). **(E)** Intraperitoneal glucose tolerance test (IPGTT), **(F)** oral glucose tolerance test (OGTT), **(G)** insulin tolerance test (ITT), and **(H)** glucagon challenge (GC) test at 8-12 months; bar graphs quantify area under the curve (n=5 to 11). Values are expressed as mean ± SEM; *p<0.05, **p<0.01, ***p<0.001 by paired t-test.

**Figure 2**

**Age dependency of the *Mgat5*$^{-/-}$ phenotype in female mice- (A)** IPGTT and **(B)** GC tests in female mice at 6 months of age. **(C)** IPGTT, **(D)** ITT and **(E)** GC of the same group of mice at 1 year of age (n= 4-16). Bar graphs are area under the curve. Values are expressed as mean ± SEM; *P<0.05, **P<0.01, ***P<0.001

**Figure 3**
**Age dependency of the *Mgat5*$^{-/-}$ phenotype in male mice- (A-C)** IPGTT of the same group of *Mgat5*$^{-/-}$ and control mice at 3, 4 and 6 months of age (n= 6-13). At 6 months of age mice were tested in **(D)** OGTT, **(E)** ITT, and **(F)** GC. Bar graphs are area under the curve. Values are expressed as mean ± SEM; *P<0.05, **P<0.01, ***P<0.001

**Figure 4**
**Metabolite profiles in male *Mgat5*$^{+/+}$ and *Mgat5*$^{-/-}$ livers (A)** Hepatic glycogen content in 8-12 month male mice (n=4 to 5). Hepatic **(B)** amino acids, **(C)** glycolysis metabolites and **(D)** hexosamine biosynthetic pathway (HBP) measured by LC-MS/MS (n=3) and expressed as fold change in mutant relative to wild type. Values are mean ± SEM; *p<0.05, **p<0.01, ***p<0.001

**Figure 5**
**N-glycosylation and cell surface expression in hepatocytes- (A)** Western blot analysis of endogenous Gcgr from liver lysates with and without PNGaseF pre-treatment of lysates (n=2). The apparent molecular weight of Gcgr was reduced by ~5kD in *Mgat5*$^{-/-}$ hepatocytes (marked a,b) consistent with the absence of the Mgat5-dependent β1,6GlcNAc branch and its extension (see Figure 1A). **(B)** Western blot for Flag-Gcgr expressed in CHO (wt), Mgat1 (Lec1) and Mgat5 (Lec4) mutants CHO cell lines reveals that both enzymes contribute to N-glycan mass on the receptor. The wild type is N-glycans are preferred substrates for further extension of branches, resulting in the broad distribution of Gcgr in the gel. **(C)** Flag-Gcgr mutations at each of the five NXS/T site were transiently expressed in HEK293 cells and analyzed by Western blotting and anti-Flag antibodies. Arrows point to early intermediates of Gcgr processing, where a shift is apparent, consistent with loss of single sites in the mutants. **(D)** Activity of Flag-Gcgr mutants was measured by transient transfection in HEK293 cells, and after 48 h cells were stimulated with glucagon for 10 min. cAMP was measured by LC-MS/MS, and the results were expressed a fraction of the response to forskolin, a chemical activator of adenylyl cyclase.

**Figure 6**
**Glucagon signaling in primary hepatocytes- (A)** Glucagon-dependent induction of cAMP in hepatocytes **(B)** cAMP concentrations following 100 μM forskolin stimulation of adenylyl cylcase for 10 min (n=7-9). **(C)**Glucose secretion by primary hepatocytes stimulated with 20 nM glucagon for the indicated times, and **(D)** glucose remaining in the cell lysate (n= 6-7). Values are expressed as mean ± SEM; *p<0.05, **p<0.01, ***P<0.001

**Figure 7**
**Characterization of hepatocyte Gcgr- (A)** Cell surface biotinylated-Gcgr in extracts of *Mgat5*$^{+/+}$ and *Mgat5*$^{-/-}$ hepatocytes (n=3) by Western blotting with anti-Gcgr antibody. **(B)** Quantification of Gcgr normalized to cadherin, mean ± SEM, (ns) not significant. **(C)** Competitive glucagon binding assays with *Mgat5*$^{+/+}$ and *Mgat5*$^{-/-}$ liver membrane preparations (n=4), and *Gcgr*$^{-/-}$ liver membranes (n=2). Curve fitting $R^2$>0.91 and 95% confidence intervals suggesting affinities were non-overlapping. **(D)** Insulin binding assay with membrane preparations from *Mgat5*$^{-/-}$ and control mice to determine quality of membranes as described in experimental procedure. Data are mean values ± SEM. **(E)** Gene array data of galectin gene family expression in mouse liver generated by the Consortium of Functional Glycomics and

reproduced with permission from Dr. J. Esko (45). **(F)** Immunoprecipitation of RFP-galectin-9 transiently expressed in primary hepatocytes, pre-treated with (+) or without (-) lactose. Western blots probed for Gcgr, RFP-galectin-9 complex and galectin-9.

**Figure 8**

**FRAP analysis of GFP-Gcgr mobility in *Mgat5*$^{+/+}$ and *Mgat5*$^{-/-}$ mice primary hepatocytes-** **(A)** Images taken from a time-lapsed series showing the target area marked by the red square, before photobleaching (prebleach), immediately after photobleaching (bleach) and after recovery (55s). **(B)** Time course of fluorescence recovery normalized to the pre-bleach intensity and graphed as fractional total recovery (n=5). **(C)** Bar graph of $t_{1/2}$ for recovery, mean ± SEM; *p<0.05, **p<0.01, ***p<0.001. **(C,D)** FRAP analysis of GFP-Gcgr transiently expressed in primary hepatocytes. Cells were treated as indicated with either 30 mM lactose, 100 μM castanospermine, 20 mM GlcNAc prior to FRAP analyses, or co-transfected with RFP-galectin-9 as described in experimental procedures. FRAP half-life ($t_{1/2}$) represent a minimum of 4-5 animals in independent experiments in which 6-10 cells were bleached. Values are expressed as mean ± SEM; *p<0.05, **p<0.01, ***p<0.001.

**Figure 9**

**Gcgr signaling is dependent on N-glycan branching and HBP. (A)** cAMP levels in primary hepatocytes pre-treated overnight with and without 20 mM GlcNAc, then stimulated with 10 nM glucagon or 100 μM forskolin for 10 min as described in experimental procedure. cAMP levels are normalized to non-treated hepatocytes and expressed as mean fold change ± SEM; *p<0.05, **p<0.01, ***p<0.001 (n=5). **(B)** HBP metabolites in *Mgat5*$^{+/+}$ and *Mgat5*$^{-/-}$ hepatocytes with and without GlcNAc treatment were measured by LC-MS/MS. **(C)** HEK293 cells with a FlpInTRex integrated tetracycline-inducible human Mgat5 were transiently transfected with Gcgr. After 48h with or without 1ug/ml tet and 20 mM GlcNAc treatment, cells were stimulated with 10 nM glucagon for 10 min, and cAMP was measured by LC-MS/MS. **(D)**HBP metabolites in HEK293 tet-Mgat5 cells measured by LC-MS/MS. **(E)** Mgat5-dependent N-glycan branching measured by Phaseolus vulgaris leucoagglutinin (L-PHA) lectin staining.

**Figure 10**

**GlcNAc supplementation enhances the glucagon response *in vivo*. (A,B)** GC tests and **(C,D)** IPGTT at 8 months of age. Bar graphs are area under the curve. Values are expressed as mean ± SEM; *p<0.05, **p<0.01, ***p<0.001. *Mgat5*$^{+/+}$ and *Mgat5*$^{-/-}$male mice at 3 weeks of age were provided a high fat diet ± GlcNAc in the drinking water as described in experimental procedure (n=3-5 per group). **(E,F)** Hepatic metabolite levels normalized to non-treated animals, and the y-axis is plotted as fold change. Values are expressed as mean ± SEM (n=3-5 mice); *p<0.05 by student t test, and the treated and control in both genotype differed, p<0.003 by 2-way ANOVA.

**Figure 11**

**A model of metabolic feedback via HBP and N-glycan branching**. In the fed state (1), hepatic glucose transport into the cell and (2), flux to HBP increases intracellular UDP-GlcNAc supply to the medial Golgi. (3), UDP-GlcNAc is a rate limiting substrate for the Mgat enzymes and, (4) N-glycan branching on Gcgr and other glycoproteins increases (left to right); (5), equilibrium shifts in a cyclical manner with feeding and fasting. Mgat5 N-glycan branching enhances galectin-9 binding and sensitivity to glucagon. The galectin lattice may promote Gcgr receptor

dimerization and/or recruit co-receptors. Increasing Gcrg sensitivity during feeding may be an adaptation that precedes and anticipates fasting in the normal feeding/fasting cycles and (6), contribute to glucagon signaling in the hyperglycemic state of diabetes. (7), High protein diet or salvage of amino acids during starvation may support UDP-GlcNAc concentrations and Gcgr sensitivity.

# Figure 1

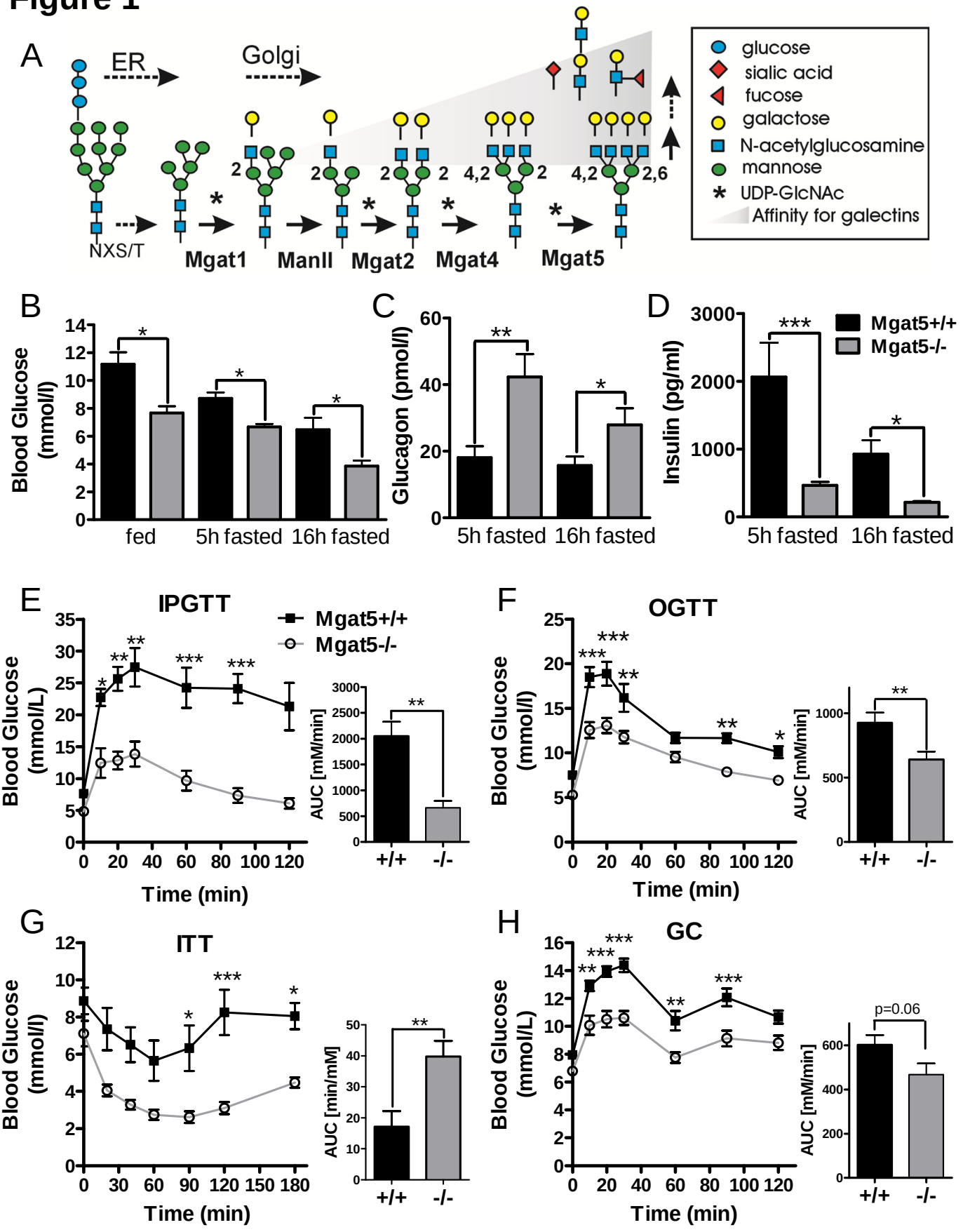

# Figure 2

## Females

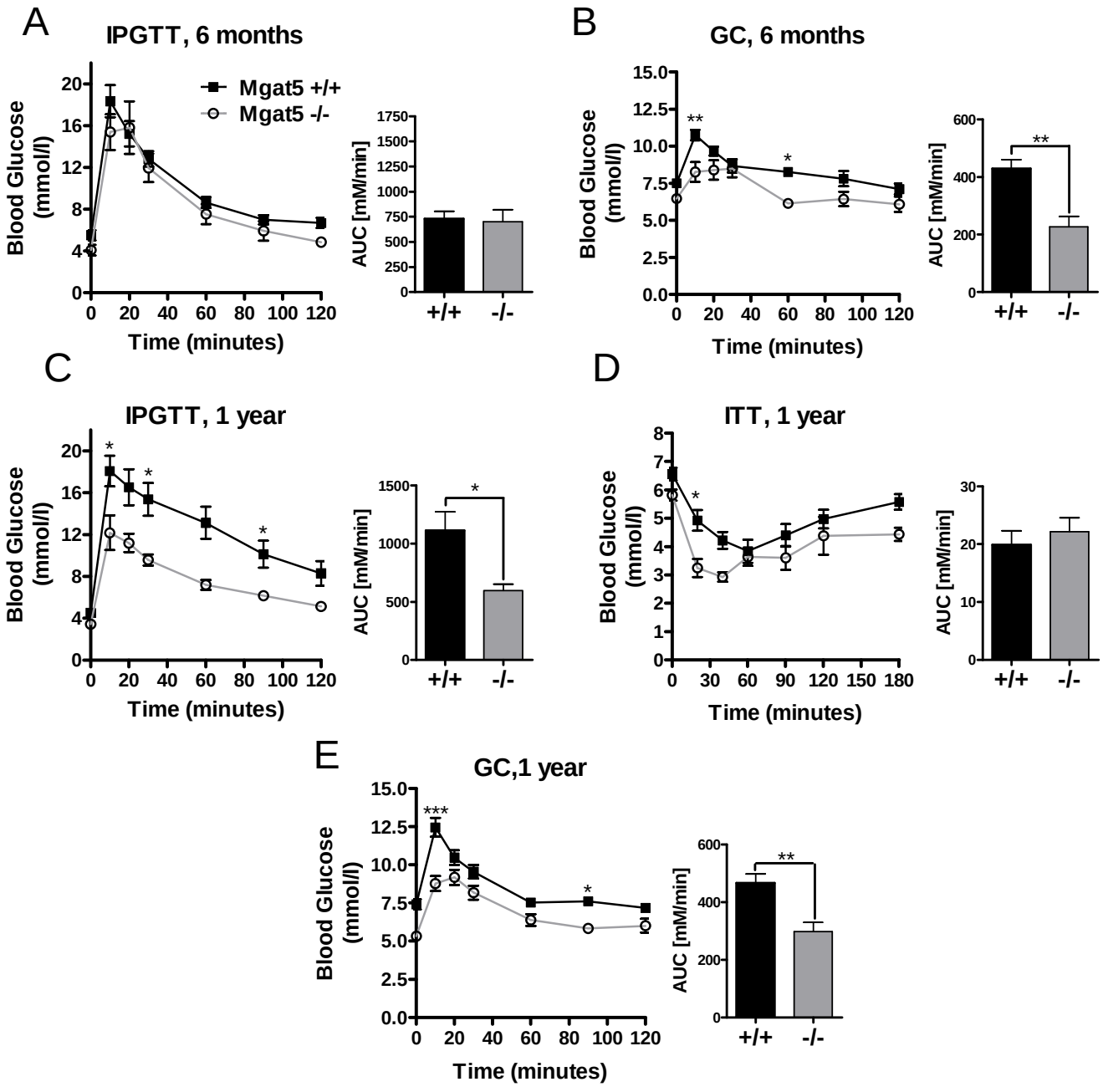

# Figure 3

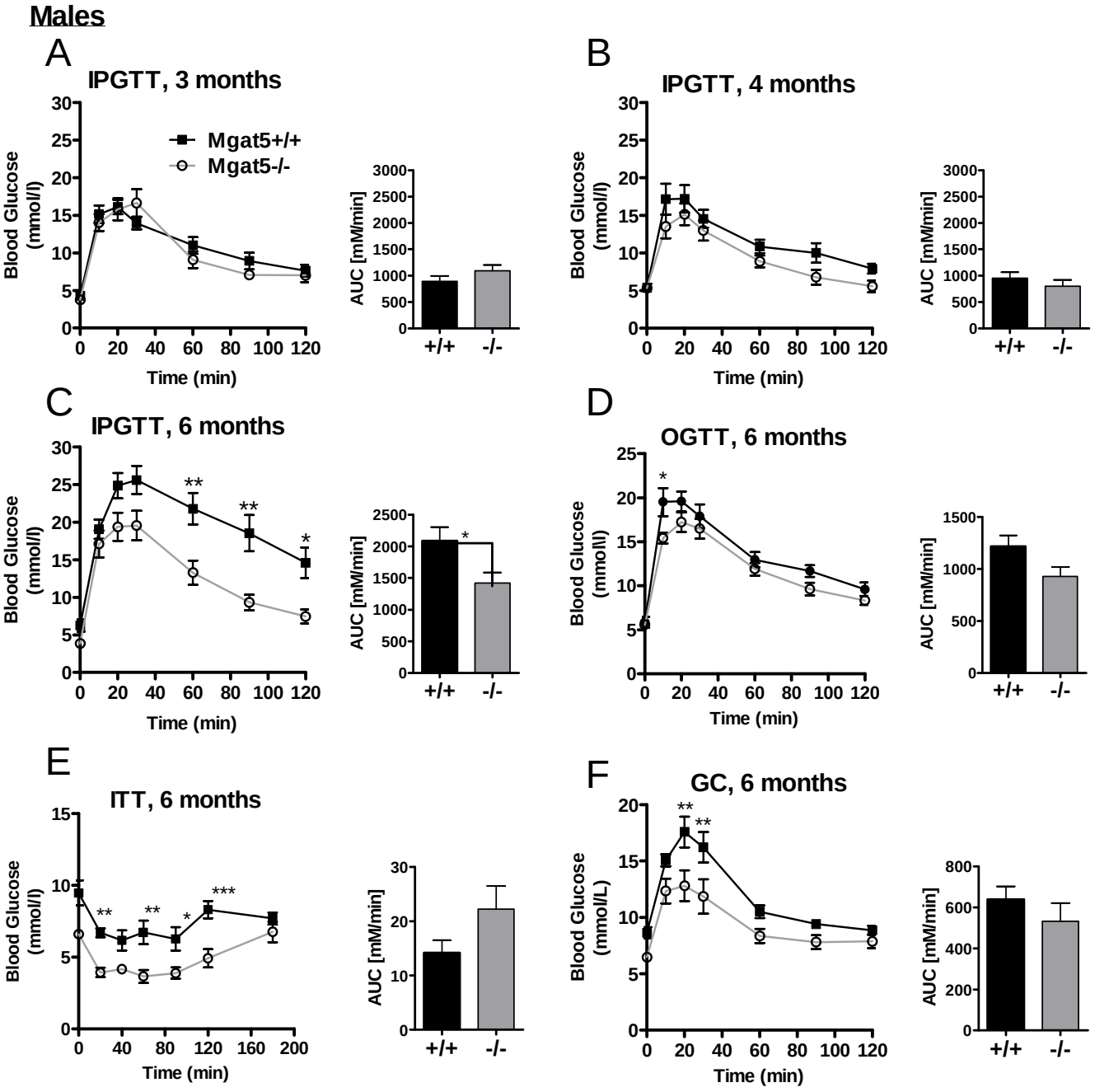

# Figure 4

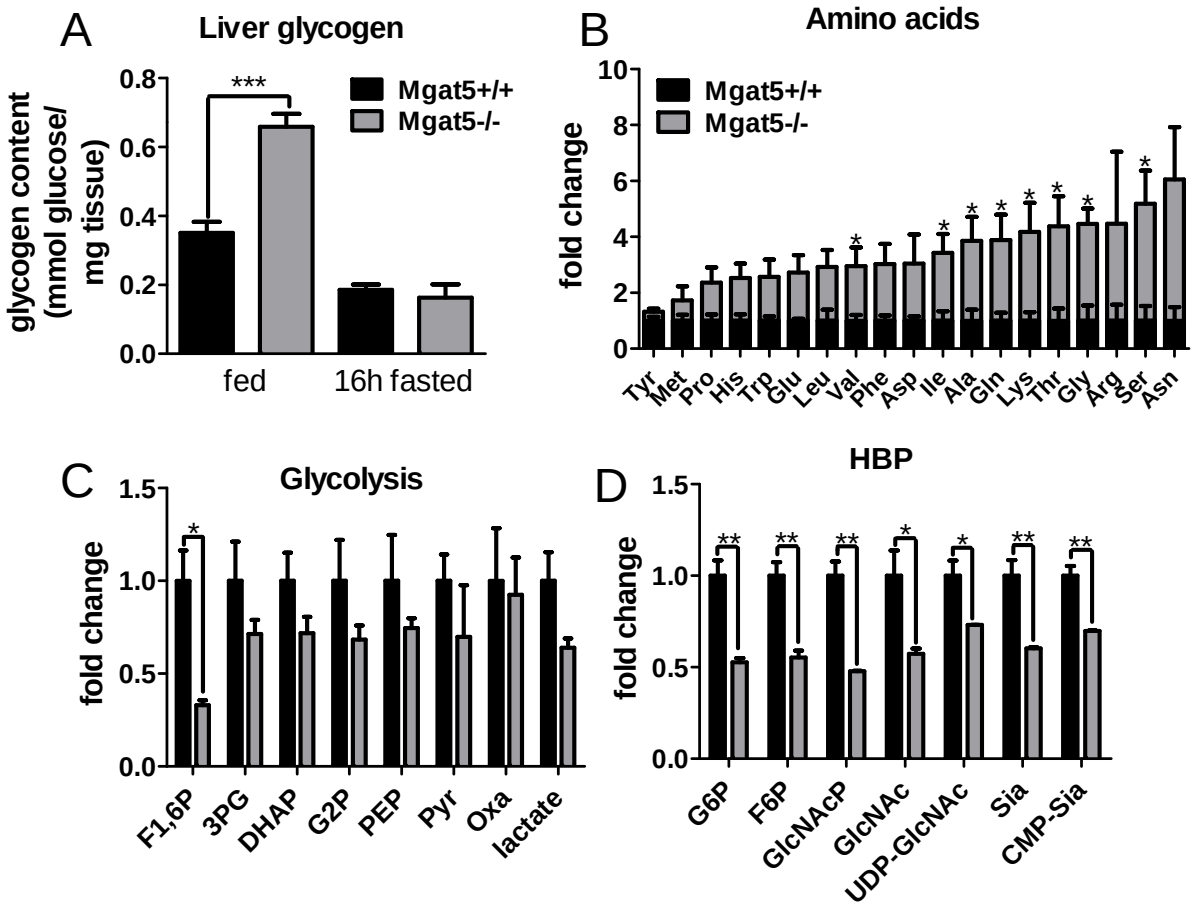

# Figure 5

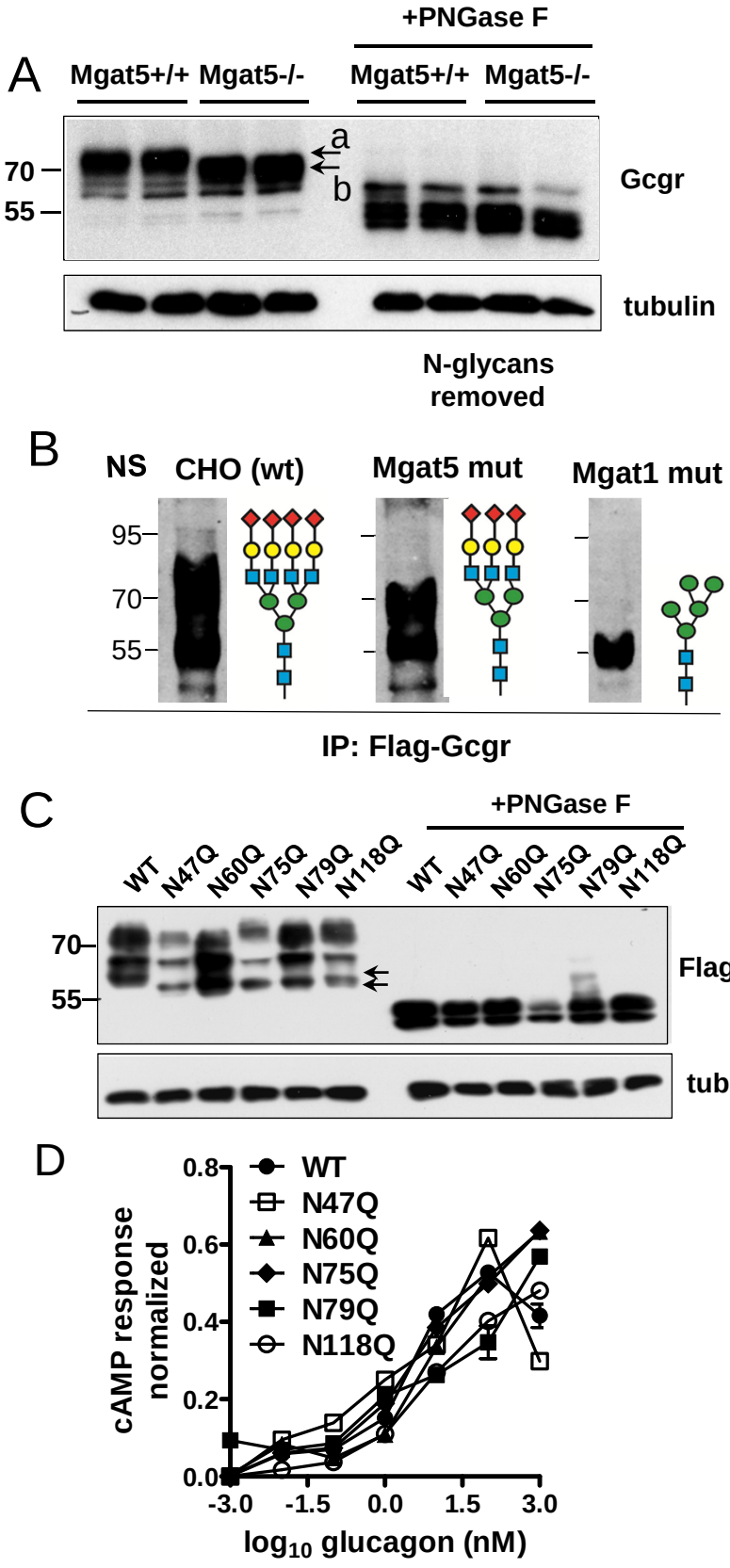

# Figure 6

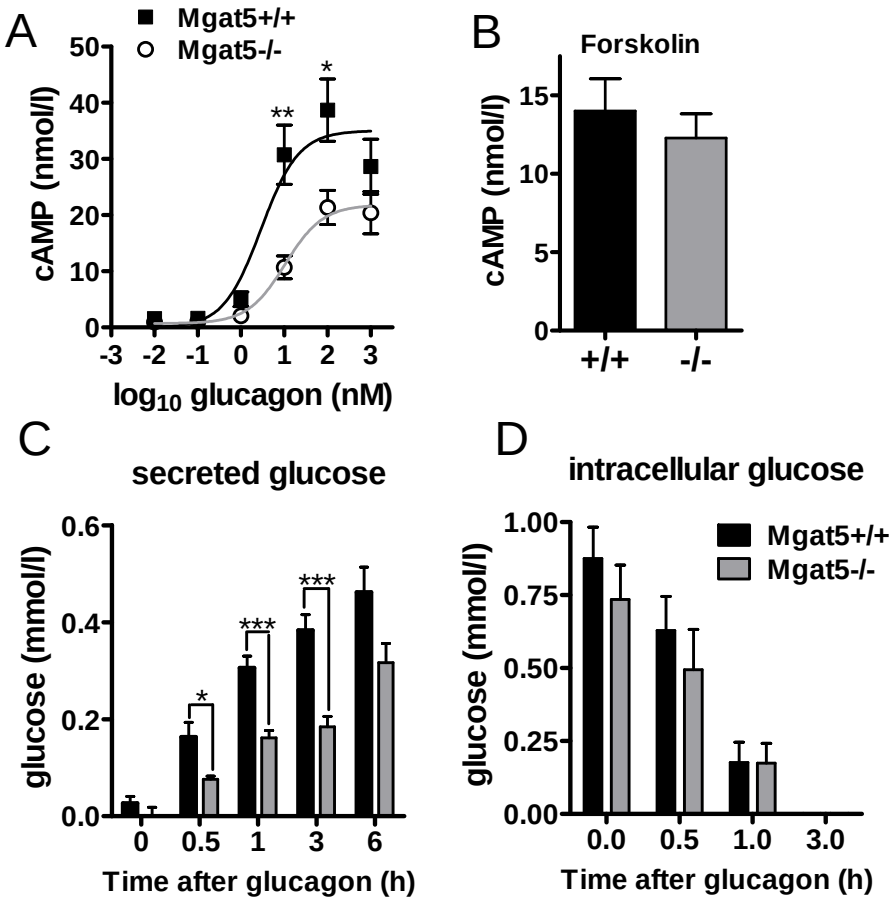

# Figure 7

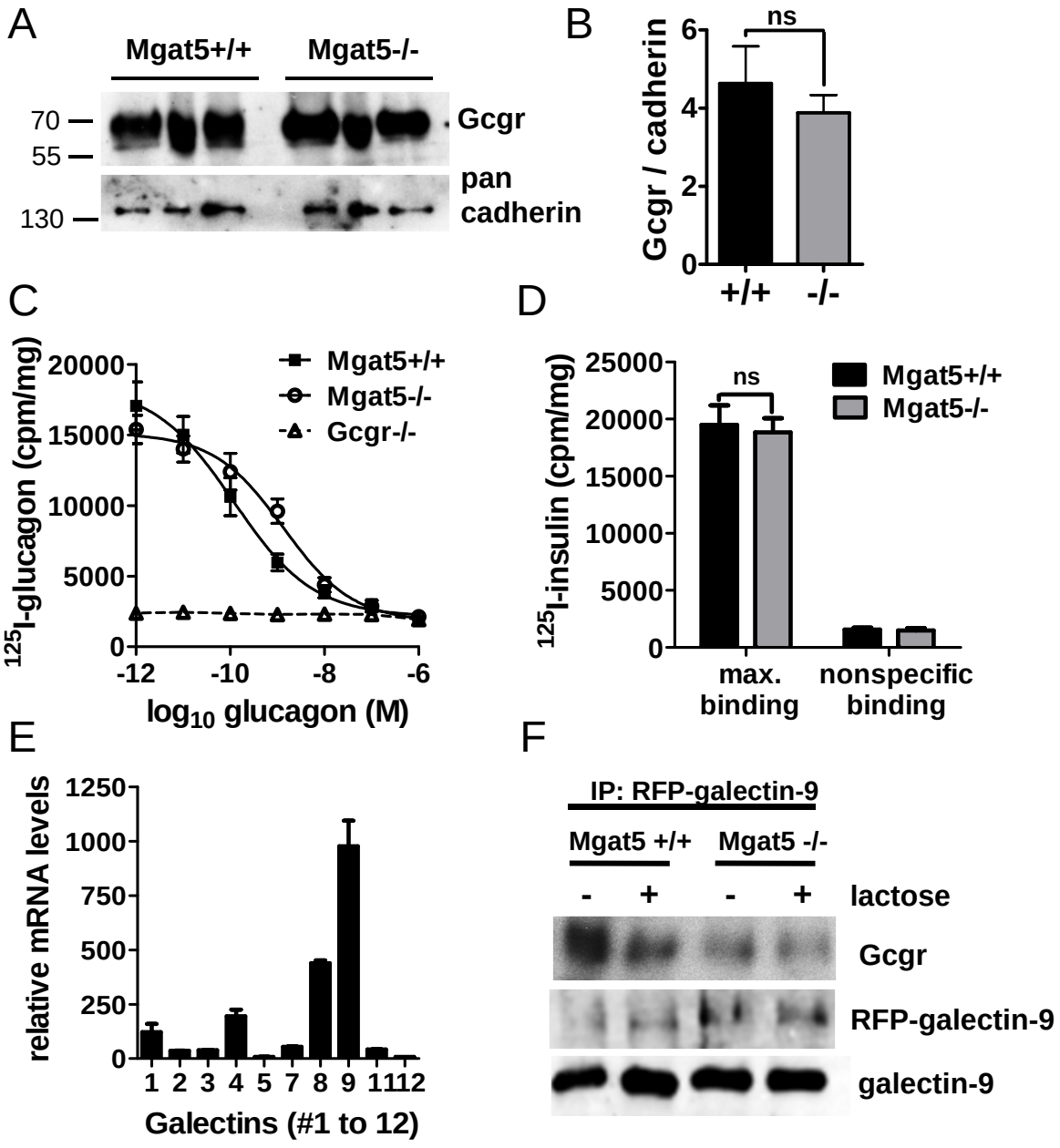

# Figure 8

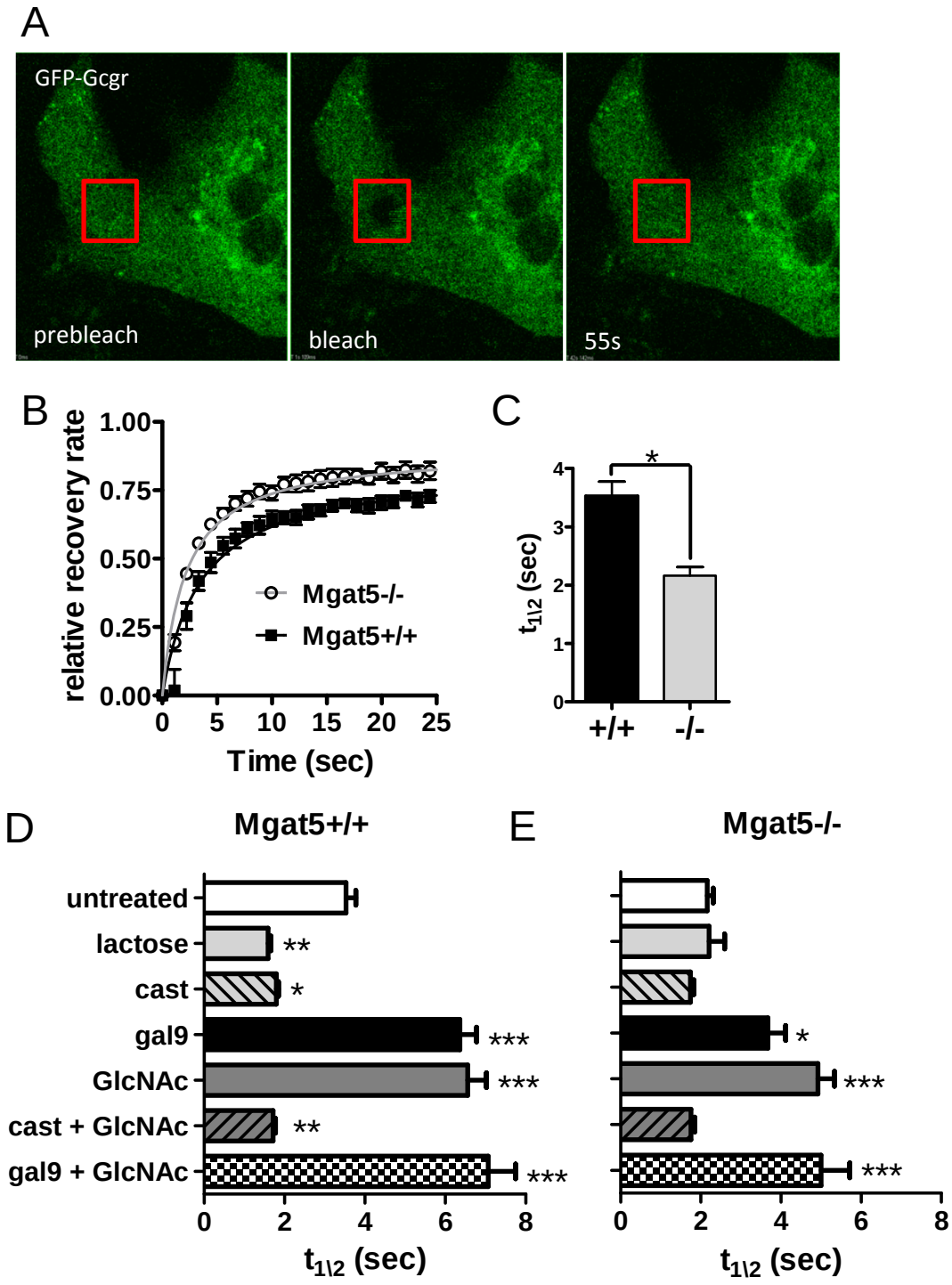

# Figure 9

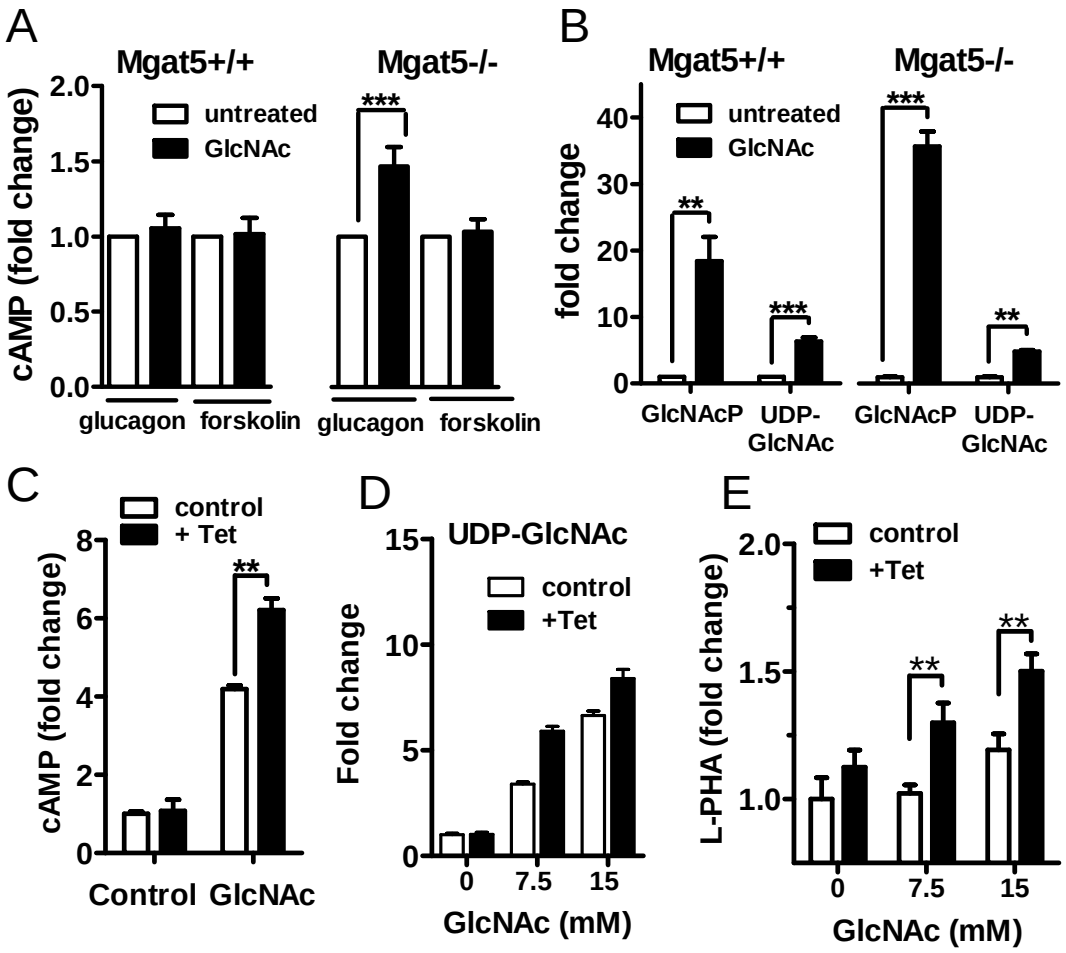

# Figure 10

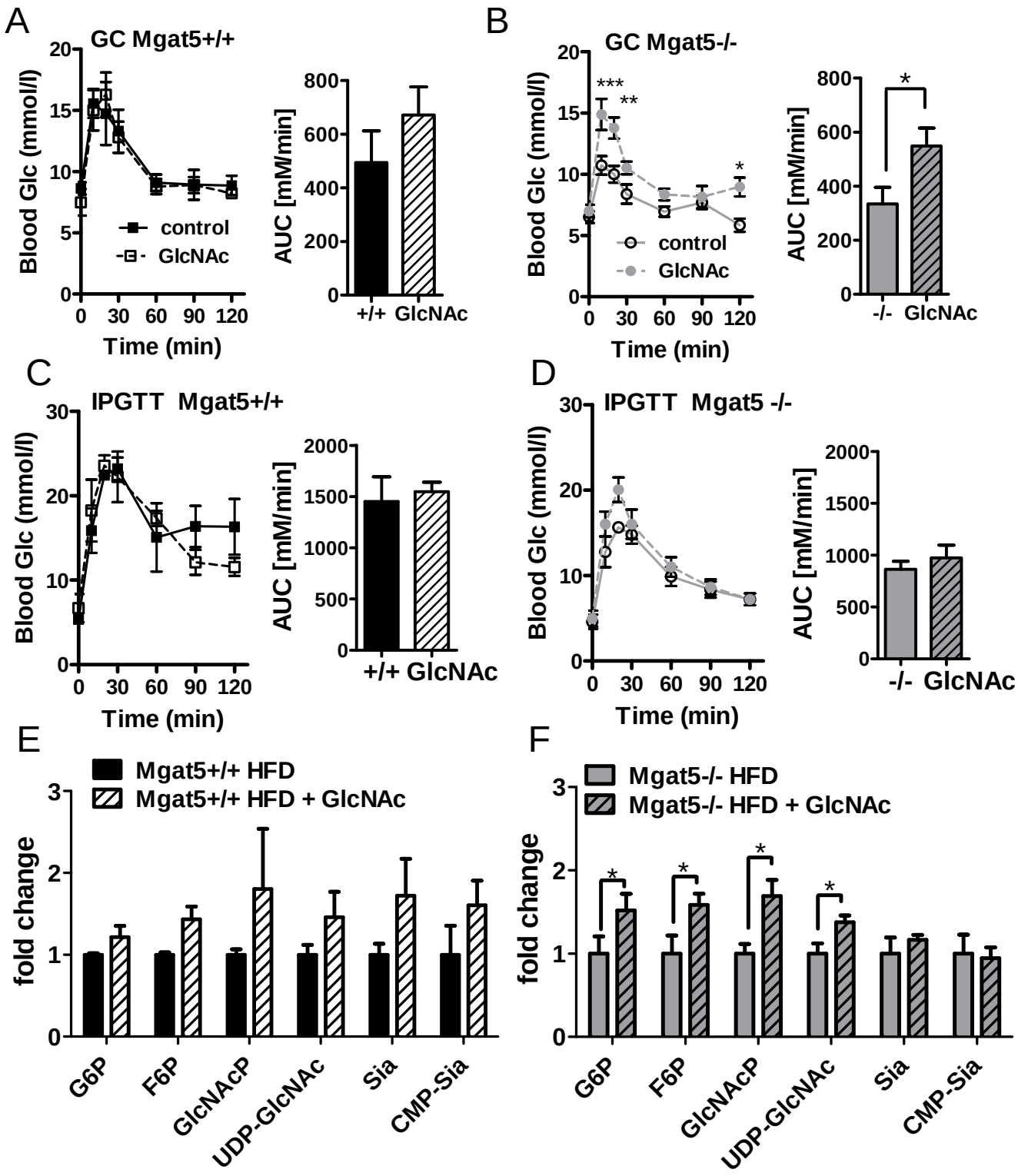

# Figure 11